On the Elastic Interaction between a Surface Step and an Edge Dislocation

Demitris Kouris, Yoshio Arai, Toru Yamaguchi and Echiro Tsuchida

Mathematics and Mechanics of Solids 2008; 13; 336
DOI: 10.1177/1081286507086905

On the Elastic Interaction between a Surface Step and an Edge Dislocation

DEMITRIS KOURIS
Department of Mechanical Engineering, University of Wyoming, Laramie, WY 82071, USA

YOSHIO ARAI
TORU YAMAGUCHI
EIICHIRO TSUCHIDA
Division of Mechanical Engineering and Science, Saitama University, Sakura-ku, Saitama, Saitama, 338-8570, Japan

Abstract: This manuscript addresses the issue of interaction between a surface step and an edge dislocation. It represents the first step in an investigation that will examine dislocation egress in the presence of surface steps. The geometric step introduces an elastic field that is altered by the presence of a dislocation in its vicinity. The complete elastic field is first determined, followed by explicit expressions for the Peach–Koehler force of the interaction. A discussion follows focusing on the possibility that an edge dislocation can be prevented from reaching the surface as a result of the field generated by the surface step. If such an outcome is possible, surface steps may be responsible for a new mechanism of strain hardening. Such a possibility has been recently suggested in the literature.

Key Words: Surface step, dislocation, Peach–Koehler force

1. INTRODUCTION

The nucleation and egress of dislocations near metallic surfaces is a topic that has received considerable attention among researchers in the field of crystal plasticity. An interesting question, first considered by Nabarro [1], is under what circumstances a dislocation can be prevented from reaching the free surface of a metal.

Nabarro concluded that, in general, the required step energy is less than the energy of the dislocation. Therefore, a clean surface will not present a barrier to dislocation egress.

A recent study by Sieradzki et al. [2] raised an intriguing issue: can existing steps on the surface prevent a dislocation from reaching it? If this is possible, a free surface can provide a new mechanism from strain hardening.

Mathematics and Mechanics of Solids **13:** 336–356, 2008 DOI: 10.1177/1081286507086905

Los Angeles, London, New Delhi and Singapore

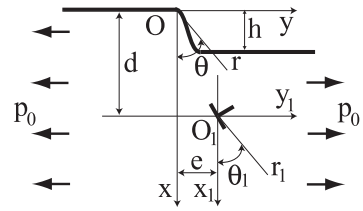

Figure 1. Surface step and edge dislocation with a Burgers vector (b_x, b_y), $\sqrt{b_x^2 + b_y^2} = b$.

A number of studies during the recent past have established the fact that surface steps interact elastically. A closed-form expression for such interaction has been recently obtained by Kukta et al. [3]. A simple calculation using this formulation appeared in [2], suggesting that the step formation required for dislocation egress might be prevented by existing steps or a vicinal surface.

In this paper, we begin an in-depth investigation of this issue by addressing first the problem of interaction between a surface step and an edge dislocation located near the surface. The geometric discontinuity due to the presence of the physical step complicates the mathematical formulation significantly. An additional complication comes from the fact that we cannot use the well-known solution of the edge dislocation in an half-plane as a part of a superposition scheme [4–9]; the physical step changes the reference geometry.

The solution we developed is expressed in the form of displacement potentials and utilizes an appropriate perturbation procedure. We first obtain the local elastic field and then determine the Peach–Koehler force, which acts on the dislocation. The sign of this force indicates whether the dislocation is attracted or repelled by the stepped surface. Our results indicate that a combination of external remote tension and appropriate material parameters allow for the existence of a region under the step where the dislocation is repelled. Specific calculations were carried out for the case of tungsten, since it can be considered isotropic. The formulation needs to be generalized if it were to address a material with cubic symmetry.

2. MATHEMATICAL DESCRIPTION OF THE PROBLEM

Let us consider an edge dislocation in the vicinity of a surface step. The step has a height h and is parallel to the dislocation line, as shown in Figure 1. Its location coincides with the center of the x, y coordinate system, while a local x_1, y_1 system refers to the position of the dislocation.

The geometric step introduces an elastic field that depends on the dipole, $h\omega$, and a concentrated moment, $h\tau$ [10, 11], where τ refers to the surface stress and ω to a dipole strength that is best determined through atomistics [12].

Traction-free conditions along the stepped surface, $x = 0, y < 0$ and $x = h, y > 0$ require that

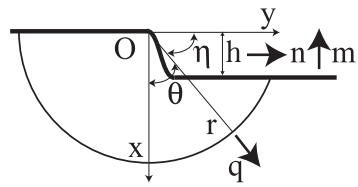

Figure 2. Geometry of a surface step with height equal to h.

$$\begin{aligned}(\sigma_{xx})_{x=0,y<0} &= 0, \quad (\sigma_{xy})_{x=0,y<0} = 0, \quad (\sigma_{xx})_{x=h,y>0} = 0,\\ (\sigma_{xy})_{x=h,y>0} &= 0. \end{aligned} \tag{1}$$

There is a uniform tension far from the step and dislocation, p_0, and a net moment, equal to $-h\tau$. This moment is present as a result of the surface stress. Consequently, the resultant force over any closed surface should vanish.

Equilibrium requirements around the step yield two conditions, one for the resultant force and one for the resultant moment:

$$\int_{-\pi/2}^{\cos^{-1} h/r} \sigma_{ij} q_j r \mathrm{d}\theta = 0, \tag{2}$$

$$\epsilon_{lik} \int_{-\pi/2}^{\cos^{-1} h/r} r q_k \sigma_{ij} q_j r \mathrm{d}\theta = -h\tau, \tag{3}$$

where q_j is a unit vector in the direction of r, as shown in Figure 2, and ϵ_{lik} is the permutation tensor. The summation convention is followed for repeated indices.

Around the dislocation, equilibrium requires that

$$\int_0^{2\pi} \sigma_{i_1 j_1} q_{j_1} r_1 \mathrm{d}\theta_1 = 0, \tag{4}$$

where q_{j_1} is a unit vector in the direction of r_1.

The displacement discontinuity associated with the dislocation is described by

$$(u_{r_1})_{\theta_1 = \frac{5}{2}\pi} - (u_{r_1})_{\theta_1 = \frac{\pi}{2}} = b_i, \tag{5}$$

where b_i denotes the Burgers vector, with components normal or parallel to the free surface.

3. METHOD OF SOLUTION

3.1. The Perturbation Methodology

The presence of the geometric step introduces a considerable complication when one attempts to determine the elastic field. The well-known solutions for the surface forces/moments and the dislocation cannot be superimposed. The problem can be solved using a perturbation method very similar to the one described in [11]. According to this approach, the total stress field due to the actual (geometric) surface step and the edge dislocation can be expressed through a summation which incorporates the stress of the corresponding plane free surface (no geometric step) and the perturbations introduced by the step

$$\sigma_{ij} = \sigma_{ij}^{(0)} + \sigma_{ij}^{(1)} + \sigma_{ij}^{(2)} + \cdots . \tag{6}$$

In this expression, $\sigma_{ij}^{(0)}$ refers to the superposition of the stress fields due to the edge dislocation, the far-field uniform tension, as well as the dipole and the concentrated moment representing the self-stress of the step (an approximation introduced in [10]), in a semi-infinite body with a plane free surface. The perturbations are assumed small when compared to the field corresponding to $\sigma_{ij}^{(0)}$. Following this methodology, the total stress can be expressed as

$$\sigma_{ij}(r,\theta) = \sigma_{ij}^{(0)}(r,\theta) + \frac{h}{r}\bar{\sigma}_{ij}^{(1)}(r,\theta) + \left(\frac{h}{r}\right)^2 \bar{\sigma}_{ij}^{(2)}(r,\theta) + \cdots , \tag{7}$$

where $\bar{\sigma}_{ij}^{(k)}(r,\theta) = \bar{T}_{ij}^{(k)}(r,\theta) + \ln\frac{h}{r}\bar{L}_{ij}^{(k)}(r,\theta)$, $\bar{T}_{ij}^{(k)}(r,\theta)$ and $\bar{L}_{ij}^{(k)}(r,\theta)$ $(k = 1, 2, ...)$ are analytical function of r and θ as described in [11]. This expansion converges for values of $h/r \ll 1$.

Enforcing the traction-free boundary condition along the stepped surface, $x = h$, $y > 0$ yields

$$\begin{aligned}\sigma_{ij}(x &= h, y)m_j = \sigma_{ij}^{(0)}(x = h, y)m_j + \frac{h}{r}\bar{\sigma}_{ij}^{(1)}(x = h, y)m_j \\ &+ \left(\frac{h}{r}\right)^2 \bar{\sigma}_{ij}^{(2)}(x = h, y)m_j + \cdots = 0,\end{aligned} \tag{8}$$

where m_j is the outward normal to the stepped surface, $x = h$, as shown in Figure 2.

The stress $\bar{\sigma}_{ij}^{(k)}(x = h, y)$ can be expressed in polar coordinates (r, θ) and expanded in a Taylor series around $\eta = 0$:

$$\bar{\sigma}_{ij}^{(k)}(r,\eta) = \bar{\sigma}_{ij}^{(k)}(r,\eta = 0) + \left(\frac{\partial\bar{\sigma}_{ij}^{(k)}(r,\eta)}{\partial\eta}\right)_{\eta=0}\eta + \left(\frac{1}{2}\frac{\partial^2\bar{\sigma}_{ij}^{(k)}(r,\eta)}{\partial\eta^2}\right)_{\eta=0}\eta^2 + \cdots , \tag{9}$$

where $k = 1, 2, \ldots$, $\eta = \pi/2 - \theta$ as shown in Figure 2. Substituting the expanded $\bar{\sigma}_{ij}^{(k)}(x = h, y)$ into the boundary condition along the stepped surface, $x = h$, $y > 0$ and considering that η is small, so that $\eta = \sin^{-1}\frac{h}{r} \cong \frac{h}{r}$, Equation (8) yields

$$\left(\sigma_{ij}^{(0)}(r,\eta)\right)_{\eta=0} m_j + \frac{h}{r}\left\{\left(\frac{\partial\sigma_{ij}^{(0)}(r,\eta)}{\partial\eta}\right)_{\eta=0} + \bar{\sigma}_{ij}^{(1)}(r,\eta=0)\right\} m_j + \left(\frac{h}{r}\right)^2$$

$$\times \quad \left\{\left(\frac{1}{2}\frac{\partial^2\sigma_{ij}^{(0)}(r,\eta)}{\partial\eta^2}\right)_{\eta=0} + \left(\frac{\partial\bar{\sigma}_{ij}^{(1)}(r,\eta)}{\partial\eta}\right)_{\eta=0} + \bar{\sigma}_{ij}^{(2)}(r,\eta=0)\right\} m_j + \cdots = 0. \quad (10)$$

As a result of this identity, the following relations are deduced:

$$\sigma_{ij}^{(0)}(r,\eta=0)m_j = 0, \quad (11)$$

$$\left\{\left(\frac{\partial\sigma_{ij}^{(0)}(r,\eta)}{\partial\eta}\right)_{\eta=0} + \bar{\sigma}_{ij}^{(1)}(r,\eta=0)\right\} m_j = 0, \quad (12)$$

$$\left\{\left(\frac{1}{2}\frac{\partial^2\sigma_{ij}^{(0)}(r,\eta)}{\partial\eta^2}\right)_{\eta=0} + \left(\frac{\partial\bar{\sigma}_{ij}^{(1)}(r,\eta)}{\partial\eta}\right)_{\eta=0} + \bar{\sigma}_{ij}^{(2)}(r,\eta=0)\right\} m_j = 0. \quad (13)$$

The first relation corresponds to the traction free condition along $x = 0$, $y \neq 0$. This condition has already been met, since the zeroth-order solution corresponds to a semi-infinite body with a plane free surface including an edge dislocation, remote tension, a dipole, and a concentrated moment, as shown in Figures 3(a–c).

If we multiply the second equation by h/r and the third equation by $(h/r)^2$, we arrive at

$$\left\{\frac{h}{r}\left(\frac{\partial\sigma_{ij}^{(0)}(r,\eta)}{\partial\eta}\right)_{\eta=0} + \frac{h}{r}\bar{\sigma}_{ij}^{(1)}(r,\eta=0)\right\} m_j = 0, \quad (14)$$

$$\left\{\left(\frac{h}{r}\right)^2\left(\frac{1}{2}\frac{\partial^2\sigma_{ij}^{(0)}(r,\eta)}{\partial\eta^2}\right)_{\eta=0} + \left(\frac{h}{r}\right)^2\left(\frac{\partial\bar{\sigma}_{ij}^{(1)}(r,\eta)}{\partial\eta}\right)_{\eta=0}\right.$$

$$+ \quad \left.\left(\frac{h}{r}\right)^2\bar{\sigma}_{ij}^{(2)}(r,\eta=0)\right\} m_j = 0. \quad (15)$$

These expressions for the first- and the second-order perturbations on $x = 0$, $y > 0$ lead to the equivalent tractions $p_i^{(1)}$ and $p_i^{(2)}$, which can be applied at the semi-infinite body with a plane surface. These tractions are given by

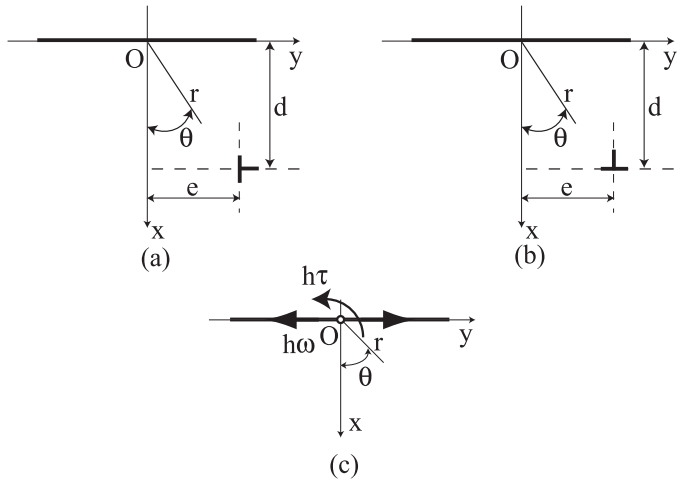

Figure 3. (a) An edge dislocation near a plane surface, with a Burgers vector $b_x = b, b_y = 0$. (b) An edge dislocation near a plane surface, with a Burgers vector $b_x = 0, b_y = b$. (c) The simplified model: a surface step represented by a dipole and a concentrated moment on a plane surface.

$$p_i^{(1)} = \sigma_{ij}^{(1)}(r, \eta = 0)m_j = -\frac{h}{r}\left(\frac{\partial \sigma_{ij}^{(0)}(r, \eta)}{\partial \eta}\right)_{\eta=0} m_j, \tag{16}$$

$$p_i^{(2)} = \sigma_{ij}^{(2)}(r, \eta = 0)m_j = -\left(\frac{h}{r}\right)^2 \left(\frac{1}{2}\frac{\partial^2 \sigma_{ij}^{(0)}(r, \eta)}{\partial \eta^2}\right)_{\eta=0} m_j$$

$$- \left(\frac{h}{r}\right)^2 \left(\frac{\partial \bar{\sigma}_{ij}^{(1)}(r, \eta)}{\partial \eta}\right)_{\eta=0} m_j. \tag{17}$$

Transforming the variable η to x and y and considering $\eta = 0$ and $m_j = (-1, 0)$, we obtain

$$p_i^{(1)} = +h\left(\frac{\partial \sigma_{ix}^{(0)}}{\partial x}\right)_{x=0}, \tag{18}$$

or

$$p_i^{(1)} = -h\left(\frac{\partial \sigma_{iy}^{(0)}}{\partial y}\right)_{x=0}. \tag{19}$$

This represents the traction condition for the first-order perturbation. A similar approach can be followed for the derivation of the second-order perturbation, leading to

$$p_i^{(2)} = -\frac{h^2}{2y}\left(\frac{\partial \sigma_{ix}^{(0)}}{\partial y}\right)_{x=0} + \frac{h}{2}\left(2\frac{\partial \sigma_{ix}^{(1)}}{\partial x} + h\frac{\partial^2 \sigma_{ix}^{(0)}}{\partial x^2}\right)_{x=0}. \tag{20}$$

Equilibrium requires that

$$\int_{\sin^{-1} h/r}^{\pi} \sigma_{ij}(r,\eta) q_j r \mathrm{d}\eta = \int_0^{\pi} \sigma_{ij}(r,\eta) q_j r \mathrm{d}\eta - \int_0^{\sin^{-1} h/r} \sigma_{ij}(r,\eta) q_j r \mathrm{d}\eta = 0, \tag{21}$$

$$\begin{aligned} \epsilon_{lki} \int_{\sin^{-1} h/r}^{\pi} r q_k \sigma_{ij} q_j r \mathrm{d}\eta &= \epsilon_{lki} \int_0^{\pi} r q_k \sigma_{ij} q_j r \mathrm{d}\eta \\ &- \epsilon_{lki} \int_0^{\sin^{-1} h/r} r q_k \sigma_{ij} q_j r \mathrm{d}\eta = -h\tau. \end{aligned} \tag{22}$$

After applying the perturbation method with small η, the Taylor expansion around $\eta = 0$ yields

$$\begin{aligned} &\int_0^{\pi} \sigma_{ij}^{(0)}(r,\eta) q_j r \mathrm{d}\eta + \frac{h}{r}\left\{\int_0^{\pi} \bar{\sigma}_{ij}^{(1)}(r,\eta) q_j r \mathrm{d}\eta - \sigma_{ij}^{(0)}(r,\eta=0) n_j r\right\} \\ &+ \left(\frac{h}{r}\right)^2 \left\{\int_0^{\pi} \bar{\sigma}_{ij}^{(2)}(r,\eta) q_j r \mathrm{d}\eta - \left(\frac{\partial \sigma_{ij}^{(0)}(r,\eta)}{\partial \eta}\right)_{\eta=0} n_j r \right. \\ &\left. - \bar{\sigma}_{ij}^{(1)}(r,\eta=0) n_j r\right\} + \cdots = 0. \end{aligned} \tag{23}$$

$$\begin{aligned} &\epsilon_{lki} \int_0^{\pi} r q_k \sigma_{ij}^{(0)}(r,\eta) q_j r \mathrm{d}\eta + \frac{h}{r}\left\{\epsilon_{lki} \int_0^{\pi} r q_k \bar{\sigma}_{ij}^{(1)}(r,\eta) q_j r \mathrm{d}\eta + r^2 \sigma_{xy}^{(0)}(r,\eta=0)\right\} \\ &+ \left(\frac{h}{r}\right)^2 \left\{\epsilon_{lki} \int_0^{\pi} r q_k \bar{\sigma}_{ij}^{(2)}(r,\eta) q_j r \mathrm{d}\eta - \frac{1}{2} r^2 \sigma_{yy}^{(0)}(r,\eta=0) + \frac{1}{2} r^2 \sigma_{xx}^{(0)}(r,\eta=0) \right. \\ &\left. + \frac{1}{2} r^2 \left(\frac{\partial \sigma_{xy}^{(0)}(r,\eta)}{\partial \eta}\right)_{\eta=0} + r^2 \bar{\sigma}_{xy}^{(1)}(r,\eta=0)\right\} + \cdots = -h\tau. \end{aligned} \tag{24}$$

Each term proportional to zeroth, first, and second power of h/r should be zero:

$$\int_0^{\pi} \sigma_{ij}^{(0)}(r,\eta) q_j r \mathrm{d}\eta = 0, \tag{25}$$

$$\int_0^{\pi} \bar{\sigma}_{ij}^{(1)}(r,\eta) q_j r \mathrm{d}\eta - \sigma_{ij}^{(0)}(r,\eta=0) n_j r = 0, \tag{26}$$

$$\int_0^{\pi} \bar{\sigma}_{ij}^{(2)}(r,\eta)q_j r\,\mathrm{d}\eta - \left(\frac{\partial \sigma_{ij}^{(0)}(r,\eta)}{\partial \eta}\right)_{\eta=0} n_j r - \bar{\sigma}_{ij}^{(1)}(r,\eta=0)n_j r = 0. \tag{27}$$

Multiplying the second equation by h/r and the third equation by $(h/r)^2$ yields

$$\int_0^{\pi} \sigma_{ij}^{(1)}(r,\eta)q_j r\,\mathrm{d}\eta - h\sigma_{ij}^{(0)}(r,\eta=0)n_j = 0, \tag{28}$$

$$\int_0^{\pi} \sigma_{ij}^{(2)}(r,\eta)q_j r\,\mathrm{d}\eta - \frac{h^2}{r}\left(\frac{\partial \sigma_{ij}^{(0)}(r,\eta)}{\partial \eta}\right)_{\eta=0} n_j - h\sigma_{ij}^{(1)}(r,\eta=0)n_j = 0. \tag{29}$$

The resultant force due to $\sigma_{ij}^{(k)}$ $(k = 1, 2, \ldots)$ acting on the face of a half circle of radius $r = a$ can be substituted by a concentrated force $f_i^{(k)}$ acting anywhere along the region $r < a$. As a approached 0, the resultant force due to $\sigma_{ij}^{(k)}$, acting on the face of a half-cylinder of radius a can be represented by a concentrated force $f_i^{(k)}$ applied at the origin. We can determine the magnitude of the concentrated forces $f_i^{(1)}$ and $f_i^{(2)}$, for the first and the second-order perturbations at $x = 0$, $y = 0$ of the semi-infinite body with a plane surface, by utilizing the zeroth and first-order solutions:

$$f_i^{(1)} = -\lim_{a\to 0}\int_0^{\pi} \sigma_{ij}^{(1)}(r=a,\eta)q_j a\,\mathrm{d}\eta = -\lim_{a\to 0} h\sigma_{ij}^{(0)}(r=a,\eta=0)n_j, \tag{30}$$

$$\begin{aligned} f_i^{(2)} &= -\lim_{a\to 0}\int_0^{\pi} \sigma_{ij}^{(2)}(a,\eta)q_j a\,\mathrm{d}\eta = \lim_{a\to 0}\left[-\frac{1}{2}\left(\frac{h}{a}\right) h\sigma_{ix}^{(0)}(x=0,y=a)\right. \\ &\quad \left. - \frac{1}{2}h^2\left(\frac{\partial \sigma_{iy}^{(0)}(x,y)}{\partial x}\right)_{x=0,y=a} - h\sigma_{iy}^{(1)}(x=0,y=a)\right]. \end{aligned} \tag{31}$$

The magnitude of the concentrated moments $\epsilon_{lki}m_{ki}^{(1)}$ and $\epsilon_{lki}m_{ki}^{(2)}$, for the first and the second-order perturbations at $x = 0$, $y = 0$ (semi-infinite body with a plane surface) are obtained through a procedure similar to the one described above:

$$\epsilon_{lki}m_{ki}^{(1)} = -\lim_{a\to 0}\epsilon_{lki}\int_0^{\pi} aq_k\sigma_{ij}^{(1)}(a,\eta)q_j a\,\mathrm{d}\eta = \lim_{a\to 0} ah\sigma_{xy}^{(0)}(x=0,y=a). \tag{32}$$

$$\begin{aligned} \epsilon_{lki}m_{ki}^{(2)} &= -\lim_{a\to 0}\epsilon_{lki}\int_0^{\pi} aq_k\sigma_{ij}^{(2)}(a,\eta)q_j a\,\mathrm{d}\eta \\ &= \lim_{a\to 0}\left[-\frac{1}{2}h^2\sigma_{yy}^{(0)}(x=0,y=a) + \frac{1}{2}h^2\sigma_{xx}^{(0)}(x=0,y=a)\right. \\ &\quad \left. + \frac{1}{2}ah^2\left(\frac{\partial \sigma_{xy}^{(0)}(x,y)}{\partial x}\right)_{x=0,y=a} + ah\sigma_{xy}^{(1)}(x=0,y=a)\right]. \end{aligned} \tag{33}$$

3.2. Displacement Potentials

3.2.1. The zeroth-order perturbation field

The displacement potentials representing the elastic field around an edge dislocation in a semi-infinite body with a plane, traction-free surface (Figures 3(a) and (b)) are given in [4–14].

For an edge dislocation having the Burgers vector, $b_x = b$, $b_y = 0$,

$$[\mathrm{I}-\mathrm{b}_x]\begin{cases} \varphi_0 = dCb_x\dfrac{\kappa+1}{\kappa}\tan^{-1}\dfrac{y-e}{x-d} \\ \qquad -eCb_x\dfrac{\kappa-1}{\kappa}\left[\dfrac{1}{2}\log\{(x-d)^2+(y-e)^2\}+\dfrac{1}{\kappa}\right], \\ \varphi_1 = -Cb_x\dfrac{\kappa+1}{\kappa}\tan^{-1}\dfrac{y-e}{x-d}, \\ \varphi_2 = Cb_x\dfrac{\kappa-1}{\kappa}\left[\dfrac{1}{2}\log\{(x-d)^2+(y-e)^2\}+\dfrac{1}{\kappa}\right], \end{cases} \tag{34}$$

$$[\mathrm{II}-\mathrm{b}_x]\begin{cases} \varphi_0 = Cb_x\int_0^\infty\{\psi_1(\lambda)-d\lambda\psi_2(\lambda)\}e^{-\lambda(x-d)}\sin\{\lambda(y-e)\}\mathrm{d}\lambda, \\ \varphi_1 = Cb_x\int_0^\infty\lambda\psi_2(\lambda)e^{-\lambda(x-d)}\sin\{\lambda(y-e)\}\mathrm{d}\lambda, \end{cases} \tag{35}$$

where $C = G/(\pi(\kappa+1))$, κ is equal to $3-4\nu$, G is the shear modulus and ν is Poisson's ratio, and

$$\psi_1(\lambda) = \frac{4\lambda^2d^2-2(\kappa-1)\lambda d-(\kappa-1)}{\lambda^2\mathrm{e}^{2\lambda d}}, \tag{36}$$

$$\psi_2(\lambda) = \frac{2(2\lambda d+1)}{\lambda^2\mathrm{e}^{2\lambda d}}. \tag{37}$$

For an edge dislocation having the Burgers vector, $b_x = 0$, $b_y = b$,

$$[\mathrm{I}-\mathrm{b}_y]\begin{cases} \varphi_0 = dCb_y\dfrac{\kappa-1}{\kappa}\left[\dfrac{1}{2}\log\{(x-d)^2+(y-e)^2\}+\dfrac{1}{\kappa}\right] \\ \qquad +eCb_y\dfrac{\kappa+1}{\kappa}\tan^{-1}\dfrac{y-e}{x-d}, \\ \varphi_1 = -Cb_y\dfrac{\kappa-1}{\kappa}\left[\dfrac{1}{2}\log\{(x-d)^2+(y-e)^2\}+\dfrac{1}{\kappa}\right], \\ \varphi_2 = -Cb_y\dfrac{\kappa+1}{\kappa}\tan^{-1}\dfrac{y-e}{x-d}, \end{cases} \tag{38}$$

$$[\mathrm{II}-\mathrm{b}_y]\begin{cases}\varphi_0=-Cb_y\int_0^\infty\{\psi_1(\lambda)-d\lambda\psi_2(\lambda)\}e^{-\lambda(x-d)}\cos\{\lambda(y-e)\}\mathrm{d}\lambda,\\ \varphi_1=-Cb_y\int_0^\infty\lambda\psi_2(\lambda)e^{-\lambda(x-d)}\cos\{\lambda(y-e)\}\mathrm{d}\lambda,\end{cases}\tag{39}$$

where

$$\psi_1(\lambda) = \frac{-4\lambda^2d^2+2(\kappa+1)\lambda d-(\kappa+1)}{\lambda^2\mathrm{e}^{2\lambda d}},\tag{40}$$

$$\psi_2(\lambda) = \frac{-2(2\lambda d-1)}{\lambda^2\mathrm{e}^{2\lambda d}}.\tag{41}$$

The far-field uniform tension is represented by

$$[\mathrm{I}-\mathrm{p}_0]\begin{cases}\varphi_0=p_0\dfrac{\kappa+1}{8}\left(y^2-x^2\right),\\ \varphi_1=-p_0\dfrac{1}{2}x.\end{cases}\tag{42}$$

3.2.2. The first-order perturbation field

The displacement potentials corresponding to a dipole ([III]) and a concentrated moment ([IV]) on a semi-infinite body (Figure 3(c)) are given in [11, 12]:

$$[\mathrm{III}]\begin{cases}\varphi_1=\dfrac{h\omega}{2\pi}\dfrac{x}{x^2+y^2},\\ \varphi_2=-\dfrac{h\omega}{2\pi}\dfrac{y}{x^2+y^2},\end{cases}\tag{43}$$

$$[\mathrm{IV}]\begin{cases}\varphi_0=\dfrac{h\tau}{\pi}\tan^{-1}\dfrac{y}{x},\\ \varphi_1=\dfrac{h\tau}{2\pi}\dfrac{y}{x^2+y^2},\\ \varphi_2=\dfrac{h\tau}{2\pi}\dfrac{x}{x^2+y^2}.\end{cases}\tag{44}$$

and the ones corresponding to the distributed traction, $p_i^{(1)}$ and the concentrated force $f_i^{(1)}$ are given by [V] and [VI], respectively:

$$[\mathrm{V}]\begin{cases}\varphi_0=-\dfrac{\kappa+1}{4\pi\kappa}\int_0^\infty\lambda\cdot p_y^{(1)}\cdot\log\{x^2+(y-\lambda)^2\}\mathrm{d}\lambda,\\ \varphi_1=-\dfrac{\kappa-1}{2\pi\kappa}\int_0^\infty p_y^{(1)}\cdot\tan^{-1}\dfrac{y-\lambda}{x}\mathrm{d}\lambda,\\ \varphi_2=\dfrac{\kappa+1}{4\pi\kappa}\int_0^\infty p_y^{(1)}\cdot\log\{x^2+(y-\lambda)^2\}\mathrm{d}\lambda.\end{cases}\tag{45}$$

$$[\mathrm{VI}]\begin{cases}\varphi_1 = -\dfrac{\kappa-1}{2\pi\kappa} f_y^{(1)} \cdot \tan^{-1}\dfrac{y}{x}, \\ \varphi_2 = \dfrac{\kappa+1}{4\pi\kappa} f_y^{(1)} \cdot \log(x^2+y^2).\end{cases} \tag{46}$$

The form of distributed traction, $p_y^{(1)}$, and the concentrated force, $f_y^{(1)}$, depends on the direction of the Burgers vector.

For an edge dislocation with a Burgers vector $(b_x, 0)$, these quantities are

$$p_y^{(1)} = -16Cb_x hd^2 \frac{d^2 - 3(\lambda-e)^2}{\{d^2+(\lambda-e)^2\}^3}, \tag{47}$$

$$f_y^{(1)} = \frac{16Cb_x hd^2 e}{\left(d^2+e^2\right)^2}. \tag{48}$$

For an edge dislocation with a Burgers vector $(0, b_y)$, they become

$$p_y^{(1)} = 32Cb_y hd \frac{(\lambda-e)\{d^2-(\lambda-e)^2\}}{\{d^2+(\lambda-e)^2\}^3}, \tag{49}$$

$$f_y^{(1)} = \frac{16Cb_y hde^2}{\left(d^2+e^2\right)^2}. \tag{50}$$

In the case of a far field, uniform tension, the corresponding traction and force are

$$p_y^{(1)} = 0, \tag{51}$$

$$f_y^{(1)} = -hp_0. \tag{52}$$

3.2.3. The second-order perturbation field

The second-order representation of the tractions ([VII]), concentrated force ([VIII]) and concentrated moment ([IX]) are

$$[\mathrm{VII}]\begin{cases}\varphi_0 = -\dfrac{\kappa+1}{4\pi\kappa}\int_0^\infty \lambda \cdot p_y^{(2)} \cdot \log\{x^2+(y-\lambda)^2\}\mathrm{d}\lambda, \\ \varphi_1 = -\dfrac{\kappa-1}{2\pi\kappa}\int_0^\infty p_y^{(2)} \cdot \tan^{-1}\dfrac{y-\lambda}{x}\mathrm{d}\lambda, \\ \varphi_2 = \dfrac{\kappa+1}{4\pi\kappa}\int_0^\infty p_y^{(2)} \cdot \log\{x^2+(y-\lambda)^2\}\mathrm{d}\lambda,\end{cases} \tag{53}$$

$$[\mathrm{VIII}]\begin{cases}\varphi_1 = -\dfrac{\kappa-1}{2\pi\kappa} f_y^{(2)} \cdot \tan^{-1}\dfrac{y}{x}, \\ \varphi_2 = \dfrac{\kappa+1}{4\pi\kappa} f_y^{(2)} \cdot \log(x^2+y^2),\end{cases} \tag{54}$$

$$[\text{IX}]\begin{cases} \varphi_0 = \dfrac{\kappa-1}{2\pi\kappa}\cdot\epsilon_{lki}m_{ki}^{(2)}\cdot\tan^{-1}\dfrac{y}{x}, \\ \varphi_1 = \dfrac{\kappa+1}{2\pi\kappa}\cdot\epsilon_{lki}m_{ki}^{(2)}\cdot\dfrac{y}{x^2+y^2}, \\ \varphi_2 = \dfrac{\kappa-1}{2\pi\kappa}\cdot\epsilon_{lki}m_{ki}^{(2)}\cdot\dfrac{x}{x^2+y^2}. \end{cases} \tag{55}$$

For a dipole and a concentrated moment,

$$p_y^{(2)} = -\frac{4h^2\omega}{\pi\lambda^3}, \tag{56}$$

$$f_y^{(2)} = \frac{2h^2\omega}{\pi a^2}, \tag{57}$$

$$\epsilon_{lki}m_{ki}^{(2)} = 0, \tag{58}$$

and for the far-field, uniform tension,

$$p_y^{(2)} = \frac{2h^2p_0}{\pi\lambda^2}, \tag{59}$$

$$f_y^{(2)} = -\frac{2h^2p_0}{\pi a}, \tag{60}$$

$$\epsilon_{lki}m_{ki}^{(2)} = -\frac{1}{2}h^2p_0, \tag{61}$$

where a is the radius of a semi-circle around the origin, as mentioned above. In order to examine convergence, the range in the integration of [V] and [VII] is assumed as (a, ∞).

The integration includes terms proportional to $1/a$, $1/a^2$ and $\log a$. By adding adequate dipole and quadrupoles, the limit $a \to 0$ can be determined in a manner similar to the one described by Kukta [11].

The solution is obtained by superposition of all the fields represented by the displacement potentials [I] to [IX]. It is a very lengthy and tedious procedure; it does not involve, however, any significant mathematical difficulties.

4. RESULTS AND DISCUSSION

After developing the complete solution for the step-dislocation interaction, the investigation focused on the Peach–Koehler force. The sign of this force dictates whether the dislocation is attracted or repelled by the surface. To simplify the calculation, the Peach–Koehler force, the material parameters for the dipole and concentrated moment, and the remote load are normalized as follows:

$$\bar{F}_i = \frac{\pi(\kappa+1)h}{b_j^2 G} F_i, \quad \Omega = \frac{(\kappa+1)\omega}{b_j G}, \quad T = \frac{(\kappa+1)\tau}{b_j G}, \quad P = \frac{(\kappa+1)hp_0}{b_j G}, \tag{62}$$

where i and j may assume the values x or y. The complete expressions of the Peach–Koehler force are given in Appendix B.

In the discussion that follows, we attempt to clarify whether or not an edge dislocation can be prevented from reaching the surface, as a result of the field generated by the surface step. Mathematically, this is done by identifying regions where the Peach–Koehler force is greater or equal to zero. If such regions exist, they will correspond to stationary locations of the dislocation.

In the expression for the Peach–Koehler force, the self-stress of the actual geometric step is represented by the term $\left(\frac{h}{r}\right)^2 f_d(\theta)$ (see equation for $\bar{F}_x$ in Appendix B). This contribution always results in attraction of the edge dislocation. The presence of remote tension, however, leads to locations of repulsive interaction, depending on the magnitude and sign of the load. The contribution of the remote tension, represented by P, is greater than the one due to surface stress, because its leading term is of order h/r, while that of the surface stress is $(h/r)^2$. As a first approximation, if we neglect terms of order higher than h/r, the normalized Peach–Koehler force $\bar{F}_x$ on the b_x dislocation is given by

$$\bar{F}_x = -\frac{h}{r}\frac{1}{\cos\theta} + 2P\frac{h}{r}\sin^2\theta\cos\theta. \tag{63}$$

It is important to note that the second term in the equation above is present as a result of the applied load "acting" on the real, geometric step. If the geometric step is not present, this term does not appear and, as a result, the Peach–Koehler force is always attractive.

The condition for repulsion, $\bar{F}_x \geq 0$, for the minimum normalized load P gives,

$$P \geq 2, \qquad \text{at } \theta = \pm\frac{\pi}{4}. \tag{64}$$

This result indicates that when $P \geq 2$, there is a region below the step where an edge dislocation is repelled, regardless of the values of Ω and T. In other words, for a high enough remote tension, the value of the surface stress and the strength of the dipole Ω do not effect the sign of the Peach–Koehler force. The depth of the stationary location is similar in magnitude to the horizontal distance between step and dislocation.

As an illustration of this result, Figure 4 shows the distribution of the normalized Peach–Koehler force, $\bar{F}_x$ on an edge dislocation with a Burgers vector perpendicular to the free surface, for $P = 2$, $\Omega = 0.335$, $T = 0.197$ (tungsten), $\alpha = 1$. For completeness, the figure includes the contributions from higher-order terms of $\left(\frac{h}{r}\right)$. The repulsive region ($\bar{F}_x > 0$) is located under the lower terrace of the step around $\theta = \pi/4$. An alternate representation of the result is shown in Figure 5. The repulsive zone between the step and dislocation is located near $d/h = e/h = 10$.

Without restricting the value of P, stationary locations for the edge dislocation can be identified through the condition:

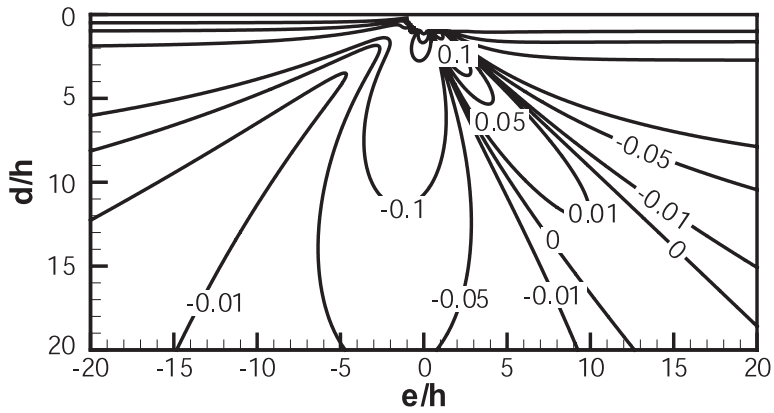

Figure 4. The normalized Peach–Koehler force, $\bar{F}_x$, on a $(b_x, 0)$ dislocation, when $P = 2$, $\Omega = 0.335$, $T = 0.197$ (tungsten), $\alpha = 1$. A repulsive region exists under the lower terrace of the step.

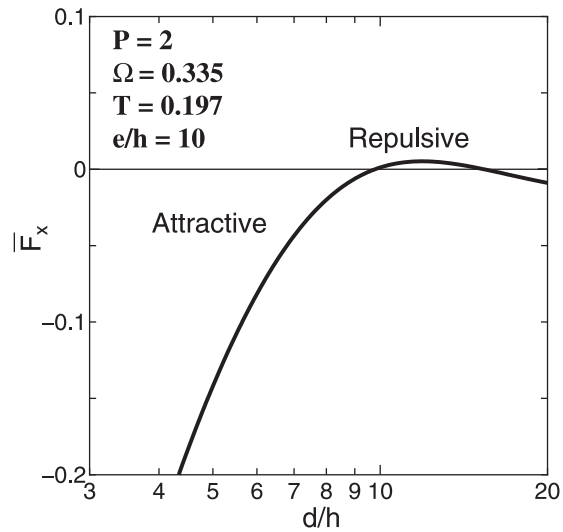

Figure 5. The normalized Peach–Koehler force, $\bar{F}_x$, acting on a $(b_x, 0)$ dislocation, as a function of the normalized distance from the surface.

$$\bar{F}_x = A_0 + A_\omega \Omega + A_\tau T = 0 \tag{65}$$

where A_0, A_τ and A_ω are given in Appendix B.

Figure 6 shows the resulting contour plot of $\bar{F}_x$, for an edge dislocation $(b_x, 0)$, as a function of the normalized dipole, Ω, and the normalized concentrated moment, T. Here $P = 2$, $r/h = 5$, $\theta = 37^\circ$, $\alpha = 1$. Materials with larger positive Ω and T tend to show the repulsive characteristics ($\bar{F}_x > 0$) for an edge dislocation under the lower terrace of the step ($\theta > 0$).

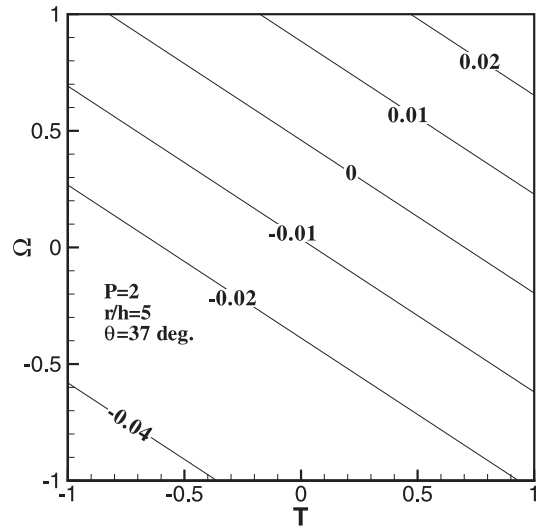

Figure 6. The normalized Peach–Koehler force, $\bar{F}_x$, acting on a $(b_x, 0)$ dislocation, when $P = 2, r/h = 5$, $\theta = 37^\circ$, $\alpha = 1$. A repulsive region ($\bar{F}_x > 0$) exists for $\Omega > 0.3$, $T > 0.3$, under the lower terrace of the step.

The values of the parameter set (Ω, T) which correspond to $\bar{F}_x = 0$ and the smallest value of $\Omega^2 + T^2$ can be found using the Lagrange multiplier λ,

$$\bar{F}_x = 0, \tag{66}$$

$$2\Omega + \lambda \frac{\partial \bar{F}_x}{\partial \Omega} = 0, \tag{67}$$

$$2T + \lambda \frac{\partial \bar{F}_x}{\partial T} = 0, \tag{68}$$

which leads to the following values:

$$T = -\frac{A_0 A_\tau}{A_\omega^2 + A_\tau^2}, \tag{69}$$

$$\Omega = -\frac{A_0 A_\omega}{A_\omega^2 + A_\tau^2}. \tag{70}$$

If we choose a moderate value of r/h, say 5.0, and $P = 2$ then we can draw the relation between (Ω, T) and θ that correspond to a Peach–Koehler force equal to zero, as shown in Figure 7. The value of the polar coordinate θ has a significant effect on the minimum combination of Ω and T. Around $\theta = \pm\pi/4$, Ω and T tend to be relatively small (smaller than ± 1) compared with other locations.

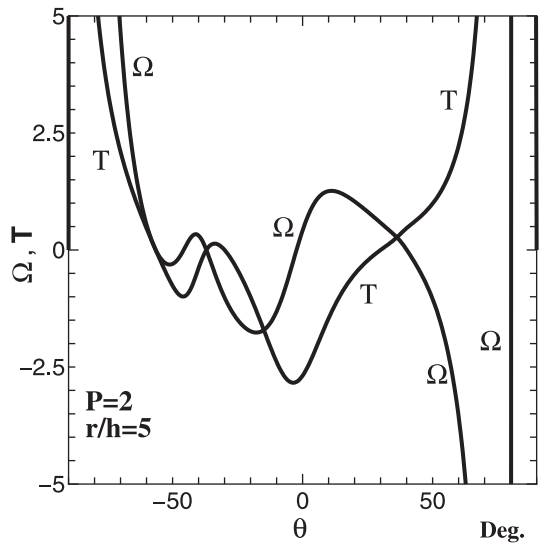

Figure 7. Relation between the normalized material parameters, (Ω, T) and θ when $\bar{F}_x = 0$, $P = 2$; the Burgers vector is perpendicular to the free surface, $(b_x, 0)$.

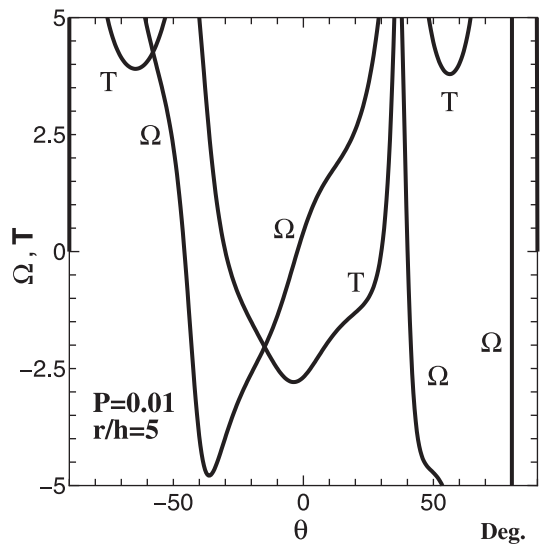

Figure 8. Relation between the normalized material parameters, (Ω, T) and θ when $\bar{F}_x = 0$, $P = 0.01$; the Burgers vector is perpendicular to the free surface, $(b_x, 0)$.

This calculation can be repeated for any values of P and r/h. Figure 8 illustrates the possible values of (Ω, T) as functions of θ that lead to zero force, for $P = 0.01$. For any

angle θ, drawing a line parallel to the (Ω, T) axis, yields the values of (Ω, T) that correspond to a Peach–Koehler equal to zero. An edge dislocation in these regions is no longer attracted by the surface.

5. CONCLUSIONS

This work addresses the problem of the elastic interaction between a surface step and an edge dislocation. The results of our investigation suggest that an edge dislocation can be repelled in certain regions near a geometric step at the surface. In the case of tungsten that we used as the template material, we found that repulsion is associated with values of P around 1 or 2. For such values of P and a remote load p_0 in the range of $100MPa$, the height h of the step must be in the order of 100 nanometers. So, it is clear that a single step on a tungsten surface will usually not stop the dislocation from approaching the surface.

The approach described here is not limited to tungsten. For smaller values of P, say in the order of 0.1 or 0.01, one can calculate Ω and T that correspond to stationary values of the Peach–Koehler force. Such calculations were performed and are illustrated in Figure 8. It is probably safe to argue, however, that a single step is an unlikely barrier to dislocation egress, at least in the case of isotropic materials.

In the introduction, we discussed that a dislocation needs enough energy not only to reach the surface but also to provide for the energy required by the corresponding step, which will be created by the dislocation egress. If this step location is near a train of existing steps, the step will be repelled. The magnitude of the interaction can be estimated using equation (8) in [3]. It can also be determined exactly using an analytical form that has not been published yet. In any case, this additional energetic requirement may be sufficient to stop the dislocation from exiting the bulk, as suggested by Sieradzki and his co-workers [2]. This will be almost certainly true if the system is subjected to a remote tension field. The next step of our investigation will attempt to provide the quantitative evidence, which will help us answer this question.

APPENDIX A. DISPLACEMENT POTENTIAL METHOD

The Papcovich–Neuber displacement potentials φ_0, φ_1 and φ_2 are given by

$$2Gu_x = \frac{\partial}{\partial x}(\varphi_0 + x\varphi_1 + y\varphi_2) - (\kappa + 1)\varphi_1 \tag{71}$$

$$2Gu_y = \frac{\partial}{\partial y}(\varphi_0 + x\varphi_1 + y\varphi_2) - (\kappa + 1)\varphi_2 \tag{72}$$

$$\nabla^2\varphi_0 = \nabla^2\varphi_1 = \nabla^2\varphi_2 = 0 \tag{73}$$

$$\nabla^2 = \frac{\partial^2}{\partial x^2} + \frac{\partial^2}{\partial y^2}. \tag{74}$$

Here, (u_x, u_y) are the displacements in the x, y directions, respectively. The Kolosov constant assumes the values $\kappa = (3-\nu)/(1+\nu)$ for plane stress and $\kappa = 3-4\nu$ for plane strain. G denotes the shear modulus and ν the Poisson's ratio.

APPENDIX B. THE PEACH–KOEHLER FORCE ON AN EDGE DISLOCATION NEAR A SURFACE STEP

For an edge dislocation with a Burgers vector $(b_x, 0)$, the components of the Peach–Koehler force are

$$\begin{aligned}
F_x &= \frac{b_x^2 G}{\pi(\kappa+1)}\left\{-\frac{1}{d}+h\left[-\frac{1}{2d^2}-\frac{1}{d^2\pi}\tan^{-1}\left[\frac{e}{d}\right]\right.\right.\\
&- \left.\left.\frac{e\left(-3d^6+53d^4e^2+11d^2e^4+3e^6\right)}{3d\left(d^2+e^2\right)^4\pi}\right]\right\}+b_x\left\{-\frac{2h\tau}{\pi}\frac{d^2\left(d^2-3e^2\right)}{\left(d^2+e^2\right)^3}\right.\\
&+ \frac{4h\omega}{\pi}\frac{de(d^2-e^2)}{\left(d^2+e^2\right)^3}+\frac{h^2\omega}{\pi^2}\frac{1}{(d^2+e^2)^4}\left[8d(-d^4+8d^2e^2-3e^4)\log\frac{\alpha h}{\sqrt{d^2+e^2}}\right.\\
&+ \left.4e(9d^4-14d^2e^2+e^4)\tan^{-1}\frac{e}{d}-8d(d^4-7d^2e^2+2e^4)\right]\\
&+ \left.\frac{h^2\omega}{\pi}\frac{1}{(d^2+e^2)^4}\cdot 2e(9d^4-14d^2e^2+e^4)\right\}+\frac{2b_x hp_0}{\pi}\frac{de^2}{\left(d^2+e^2\right)^2}\\
&- \frac{b_x h^2 p_0}{\pi}\frac{e^2\left(-3d^2+e^2\right)}{\left(d^2+e^2\right)^3}+\frac{2b_x h^2 p_0}{\pi^2}\frac{de\left(-3d^2+e^2\right)}{\left(d^2+e^2\right)^3}\\
&- \frac{2b_x h^2 p_0}{\pi^2}\frac{d^4-6d^2e^2+e^4}{\left(d^2+e^2\right)^3}\tan^{-1}\frac{e}{d}+\frac{8b_x h^2 p_0}{\pi^2}\frac{de\left(-d^2+e^2\right)}{\left(d^2+e^2\right)^3}\log\frac{\alpha h}{\sqrt{d^2+e^2}}, \quad (75)
\end{aligned}$$

and

$$\begin{aligned}
F_y &= \frac{b_x^2 G}{\pi(\kappa+1)}\frac{16d^4e^2h}{(d^2+e^2)^4\pi}+b_x\left\{-\frac{8h\tau}{\pi}\frac{d^3e}{\left(d^2+e^2\right)^3}-\frac{2h\omega}{\pi}\frac{d^2(d^2-3e^2)}{\left(d^2+e^2\right)^3}\right.\\
&- \frac{h^2\omega}{\pi^2}\frac{1}{(d^2+e^2)^4}\left[48d^2e\left(d^2-e^2\right)\log\frac{\alpha h}{\sqrt{d^2+e^2}}+12d(d^4-6d^2e^2+e^4)\tan^{-1}\frac{e}{d}\right.\\
&+ \left.\left.40d^2e\left(d^2-e^2\right)\right]-\frac{h^2\omega}{\pi}\frac{6d(d^4-6d^2e^2+e^4)}{(d^2+e^2)^4}\right\}
\end{aligned}$$

$$- \frac{2b_x h p_0}{\pi}\frac{d^2 e}{\left(d^2+e^2\right)^2} + \frac{2b_x h^2 p_0}{\pi}\frac{de\left(-d^2+e^2\right)}{\left(d^2+e^2\right)^3} + \frac{2b_x h^2 p_0}{\pi^2}\frac{d^2\left(d^2-3e^2\right)}{\left(d^2+e^2\right)^3}$$

$$+ \frac{4b_x h^2 p_0}{\pi^2}\frac{de\left(-3d^2+e^2\right)}{\left(d^2+e^2\right)^3}\tan^{-1}\frac{e}{d} + \frac{4b_x h^2 p_0}{\pi^2}\frac{d^2\left(d^2-3e^2\right)}{\left(d^2+e^2\right)^3}\log\frac{\alpha h}{\sqrt{d^2+e^2}}. \quad (76)$$

For an edge dislocation with a Burgers vector $(0, b_y)$, the components of the Peach–Koehler force are

$$\begin{aligned} F_x &= \frac{b_y^2 G}{\pi(\kappa+1)}\left\{-\frac{1}{d} + h\left[-\frac{1}{2d^2} - \frac{1}{d^2\pi}\tan^{-1}\left[\frac{e}{d}\right]\right.\right. \\ &+ \left.\left.\frac{e\left(3d^6+11d^4e^2-43d^2e^4-3e^6\right)}{3d\left(d^2+e^2\right)^4\pi}\right]\right\} + b_y\left\{-\frac{4h\tau}{\pi}\frac{de\left(d^2-e^2\right)}{\left(d^2+e^2\right)^3}\right. \\ &+ \frac{2h\omega}{\pi}\frac{e^2(3d^2-e^2)}{\left(d^2+e^2\right)^3} + \frac{h^2\omega}{\pi^2}\frac{1}{(d^2+e^2)^4}\left[-8e\left(3d^4-8d^2e^2+e^4\right)\log\frac{\alpha h}{\sqrt{d^2+e^2}}\right. \\ &- \left.4d(d^4-14d^2e^2+9e^4)\tan^{-1}\frac{e}{d} - 4e\left(7d^4-12d^2e^2+e^4\right)\right] \\ &- \left.\frac{h^2\omega}{\pi}\frac{2d(d^4-14d^2e^2+9e^4)}{(d^2+e^2)^4}\right\} + b_y p_0 + \frac{2b_y h p_0}{\pi}\frac{e^3}{\left(d^2+e^2\right)^2} \\ &+ \frac{4b_y h^2 p_0}{\pi}\frac{de^3}{\left(d^2+e^2\right)^3} + \frac{2b_y h^2 p_0}{\pi^2}\frac{d^2\left(d^2-3e^2\right)}{\left(d^2+e^2\right)^3} \\ &- \frac{4b_y h^2 p_0}{\pi^2}\frac{de\left(d^2-3e^2\right)}{\left(d^2+e^2\right)^3}\tan^{-1}\frac{e}{d} + \frac{4b_y h^2 p_0}{\pi^2}\frac{e^2\left(-3d^2+e^2\right)}{\left(d^2+e^2\right)^3}\log\frac{\alpha h}{\sqrt{d^2+e^2}}, \quad (77) \end{aligned}$$

and

$$\begin{aligned} F_y &= \frac{b_y^2 G}{\pi(\kappa+1)}\frac{16d^2e^4h}{(d^2+e^2)^4\pi} + b_y\left\{\frac{2h\tau}{\pi}\frac{d^2(d^2-3e^2)}{\left(d^2+e^2\right)^3} - \frac{4h\omega}{\pi}\frac{de\left(d^2-e^2\right)}{\left(d^2+e^2\right)^3}\right. \\ &+ \frac{h^2\omega}{\pi^2}\frac{1}{(d^2+e^2)^4}\left[8d\left(d^4-8d^2e^2+3e^4\right)\log\frac{\alpha h}{\sqrt{d^2+e^2}}\right. \\ &- \left.4e(9d^4-14d^2e^2+e^4)\tan^{-1}\frac{e}{d} + 8d\left(d^4-7d^2e^2+2e^4\right)\right] \\ &- \left.\frac{h^2\omega}{\pi}\frac{2e(9d^4-14d^2e^2+e^4)}{(d^2+e^2)^4}\right\} \end{aligned}$$

$$- \frac{2b_y h p_0}{\pi} \frac{de^2}{\left(d^2+e^2\right)^2} + \frac{b_y h^2 p_0}{\pi} \frac{e^2\left(-3d^2+e^2\right)}{\left(d^2+e^2\right)^3} - \frac{2b_y h^2 p_0}{\pi^2} \frac{de\left(-3d^2+e^2\right)}{\left(d^2+e^2\right)^3}$$

$$+ \frac{2b_y h^2 p_0}{\pi^2} \frac{d^4-6d^2e^2+e^4}{\left(d^2+e^2\right)^3} \tan^{-1}\frac{e}{d} - \frac{8b_y h^2 p_0}{\pi^2} \frac{de\left(-d^2+e^2\right)}{\left(d^2+e^2\right)^3} \log\frac{\alpha h}{\sqrt{d^2+e^2}}. \quad (78)$$

In polar coordinates, the position of a dislocation is described by $d = r\cos\theta, e = r\sin\theta$. The expression for the x-component of the Peach–Koehler force, $\bar{F}_x$, acting on an edge dislocation $(b_x, 0)$ is given by

$$\bar{F}_x = A_0 + A_\omega \Omega + A_\tau T, \quad (79)$$

where

$$A_0 = -\frac{h}{r} f_s + \left(\frac{h}{r}\right)^2 f_d + P\frac{h}{r} f_{p1} + P\left(\frac{h}{r}\right)^2 f_{p2} + P\left(\frac{h}{r}\right)^2 \log\frac{\alpha h}{r} f_{p3}, \quad (80)$$

$$A_\omega = \left(\frac{h}{r}\right)^2 f_{\omega 1} + \left(\frac{h}{r}\right)^3 f_{\omega 2} + \left(\frac{h}{r}\right)^3 \log\frac{\alpha h}{r} f_{\omega 3}, \quad (81)$$

$$A_\tau = \left(\frac{h}{r}\right)^2 f_{\tau 1}, \quad (82)$$

$$f_s(\theta) = \frac{1}{\cos\theta}, \quad (83)$$

$$f_d(\theta) = \frac{1}{24\pi} \frac{-12(\pi + 2\theta + 2\sin 2\theta) + 8\sin 6\theta + 3\sin 8\theta}{\cos^2\theta}, \quad (84)$$

$$f_{p1}(\theta) = \frac{\cos\theta - \cos 3\theta}{2} \quad (85)$$

$$f_{p2}(\theta) = \frac{1}{2\pi}\{\pi\cos 2\theta - (\pi + 4\theta)\cos 4\theta - 2\sin 2\theta - 2\sin 4\theta\} \quad (86)$$

$$f_{p3}(\theta) = -\frac{2\sin 4\theta}{\pi} \quad (87)$$

$$f_{\omega 1}(\theta) = \sin 4\theta, \quad (88)$$

$$f_\tau(\theta) = -\cos 2\theta - \cos 4\theta, \quad (89)$$

$$f_{\omega 2}(\theta) = \frac{1}{\pi}\{-3\cos 3\theta - 5\cos 5\theta + (2\theta + \pi)(\sin 3\theta + 3\sin 5\theta)\}, \quad (90)$$

$$f_{\omega 3}(\theta) = -\frac{2}{\pi}(\cos 3\theta + 3\cos 5\theta). \quad (91)$$

REFERENCES

[1] Nabarro, F. R. N. in *Surface Effects in Crystal Plasticity,* ed. R. M. Latanision and J. T. Fourie, p. 49, The Netherlands, Noordhoff, 1977.

[2] Sieradzki, K., Rinaldi, A., Friesen, C. and Peralta, P. Length scales in crystal plasticity. *Acta Materialia,* 54, 4533–4538 (2006).

[3] Kukta, R. V., Peralta, A. and Kouris, D. Elastic interaction of surface steps: effect of atomic-scale roughness. *Physical Review Letters,* 88, 186102 (2002).

[4] Head, A. K. The interaction of dislocation and boundaries. *Philosophical Magazine A,* 44, 92–94 (1953).

[5] Head, A. K. Edge dislocation in inhomogeneous media. *Proceedings of the Physical Society (London) B,* 66, 793–801 (1953).

[6] Conners, G. H. The interaction of a dislocation with a coated plane boundary. *International Journal of Engineering Science,* 5, 25–38 (1967).

[7] Weeks, R., Dundurs, J. and Stippes, M. Exact analysis of an edge dislocation near a surface layer. *International Journal of Engineering Science,* 6, 365–372 (1968).

[8] Lubarda, V. A. and Kouris, D. A. Stress fields due to dislocation walls in infinite and semi-infinite bodies. *Mechanics of Materials,* 23, 169–189 (1996).

[9] Lubarda, V. A. and Kouris, D. A. Stress fields due to dislocation arrays at interfaces. *Mechanics of Materials,* 23, 191–203 (1996).

[10] Marchenko, V. I. and Parshin, A. Ya. Elastic properties of crystal surfaces. *Soviet Physics JETP,* 52, 129–131 (1980).

[11] Kukta, R. V. and Bhattacharya, K. A micromechanical model of surface steps. *Journal of Mechanics and Physics of Solids,* 50, 615–649 (2002).

[12] Kouris, D., Peralta, A. and Sieradzki, K. Elastic interaction of defects on crystal surfaces. *Journal of Engineering Materials and Technology (Transactions of the ASME),* 121, 129–135 (1999).

[13] Tsuchida, E. and Nakahara, I. Three-dimensional stress concentration around a spherical cavity in a semi-infinite elastic body. *Bulletin of the JSME,* 13-58, 499–508 (1970).

[14] Tsuchida, E., Ohno, M. and Kouris, D. A. Effect of an inhomogeneous elliptic insert on the elastic field of an edge dislocation. *Applied Physics A,* 53, 285–291 (1991).

[15] Ibach, H. The role of surface stress in reconstruction, epitaxial growth and stabilization of mesoscopic structures. *Surface Science Reports,* 29, 193–263 (1997).

[16] Cammarata, R. C. surface and interface stress effects in thin films. *Progress in Surface Science,* 46, 1–38 (1994).